Heteronuclear Magnetisms with Ultracold Spinor Bosonic Gases in Optical Lattices

Yongqiang Li[1,2*], Chengkun Xing[3], Ming Gong[4,5,6*], Guangcan Guo[4,5,6], and Jianmin Yuan[1,7]

[1]*Department of Physics, National University of Defense Technology, Changsha 410073, China*
[2]*Hunan Key Laboratory of Extreme Matter and Applications, National University of Defense Technology, Changsha 410073, China*
[3]*Key Lab of Quantum Information (CAS), University of Science and Technology of China, Hefei 230026, China*
[4]*CAS Key Laboratory of Quantum Information, University of Science and Technology of China, Hefei 230026, China*
[5]*Synergetic Innovation Center of Quantum Information and Quantum Physics, University of Science and Technology of China, Hefei 230026, China*
[6]*Hefei National Laboratory, University of Science and Technology of China, Hefei 230088, China*
[7]*Department of Physics, Graduate School of China Academy of Engineering Physics, Beijing 100193, China*

(Received 16 December 2023; accepted manuscript online 23 January 2024)

Motivated by recent realizations of spin-1 NaRb mixtures in the experiments [*Phys. Rev. Lett.* **114**, 255301 (2015); *Phys. Rev. Lett.* **128**, 223201 (2022)], we investigate heteronuclear magnetism in the Mott-insulating regime. Different from the identical mixtures where the boson statistics only admits even parity states from angular momentum composition, for heteronuclear atoms in principle all angular momentum states are allowed, which can give rise to new magnetic phases. While various magnetic phases can be developed over these degenerate spaces, the concrete symmetry breaking phases depend on not only the degree of degeneracy but also the competitions from many-body interactions. We unveil these rich phases using the bosonic dynamical mean-field theory approach. These phases are characterized by various orders, including spontaneous magnetization order, spin magnitude order, singlet pairing order, and nematic order, which may coexist specially in the regime with odd parity. Finally we address the possible parameter regimes for observing these spin-ordered Mott phases.

DOI: 10.1088/0256-307X/41/2/026701

Large-spin atomic gases have played an important role in understanding magnetism phases in traditional condensed matter physics, which can exhibit much rich spin structures as a result of enhanced quantum fluctuations.[1] In recent years, ultracold spinor gases have been successfully realized in experiments for both bosons[2–9] and fermions,[10–13] and the corresponding physics have been widely theoretically studied, including spin mixing, dynamics and phase transitions.[14–19] Despite much theoretical and experimental efforts on large-spin ultracold atomic systems, understanding of the spin correlation and magnetism is still rather elusive,[1,20] since numerically exact approaches are lacking[15,21–24] and typical experimentally accessed temperatures are too high to explore the realm of spin ordered phases.[25,26] Recently, the experimental magnetic long-range orders are reported for antiferromagnetism[27,28] and ferromagnetism.[29] However, few studies have touched the subject of mixtures of heteronuclear spinor bosonic gases in optical lattices, where the physics seems to be even more interesting as a result of heteronuclear spin-changing processes. Actually, a system consisting of spin-1 ^{87}Rb and ^{23}Na atoms is recently realized experimentally, though without an optical lattice.[30]

In optical lattices, the large spin manifold can be realized either by atoms with large j in alkaline-earth atoms or by considering two or more small spin identical atoms.[2,31–33] For instance, two identical spin-1 bosons can form a composite spin-2 bosons from angular momentum composition. The corresponding ground-state space is five-fold degenerate (angular momentum $F = 2$ with degree of degeneracy $g = 2F + 1 = 5$) or singlet ($F = 0$ and $g = 1$) since only even parity states are allowed for bosonic statistics. Here, the rotational symmetry for identical particles ensures that the effective spin models should only allow the isotropic Heisenberg term (direct product of two spins) and their powers.

In this Letter, we focus on heteronuclear magnetism of binary mixtures of spin-1 bosonic gases in a three-dimensional (3D) optical lattice. The absence of identity restriction admits both even and odd parity quantum states, which can give rise to new magnetic phases. We are motivated by recent experimental realizations of NaRb heteronuclear atoms in Wang's group,[34–36] in which collision induced spin exchange between heteronuclear atoms is observed. We investigate the ground-state spin structures using the bosonic dynamical mean-field theory (BDMFT) approach. We find that the spin structures are not merely

*Corresponding authors. Email: li_yq@nudt.edu.cn; gongm@ustc.edu.cn
© 2024 Chinese Physical Society and IOP Publishing Ltd

determined by ground-state degeneracy, but also their many-body competitions, which induce different types of symmetry breaking magnetic phases. Various phases in the deep Mott-insulating regime are unveiled, including the spin-singlet insulator (SSI), nematic insulator (NI), cyclic (C) phase, and different types of ferromagnetic (FM) phases. These phases are characterized by a unique order parameter or by coexisting of several different order parameters. We even find an intriguing paired FM (pFM1) phase with $F = 1$, in which the nematic, ferromagnetic and singlet pairing orders coexist. Finally we discuss the possible experimental observation of these magnetic phases in the whole Mott-insulating regime.

Bose–Hubbard Model. Under the single mode approximation,[30,37–40] the 3D lattice can be described by the following generalized Bose–Hubbard (BH) model (see Ref. [41] or the Supplementary Material for details),

$$\begin{aligned}\hat{H} = &-\sum_{\langle ij\rangle,m,\sigma} t_m(b^\dagger_{im\sigma}b_{jm\sigma} + \text{H.c.}) - \sum_{i,m}\mu_m n_{im} \\ &+ \sum_{i,m}\left[\frac{1}{2}U_m n_{im}(n_{im}-1) + \frac{1}{2}U'_m(\boldsymbol{S}^2_{im} - 2n_{im})\right. \\ &\left. + U_\alpha n_{i1}n_{i2} + U_\beta \boldsymbol{S}_{i1}\cdot\boldsymbol{S}_{i2} + \frac{1}{3}U_\gamma \Theta^\dagger_i\Theta_i\right], \qquad (1)\end{aligned}$$

where $b^\dagger_{im\sigma}$ ($b_{im\sigma}$) represents the bosonic creation (annihilation) operator of hyperfine state $\sigma = \{1, 0, -1\}$ for species $m = 1, 2$ at lattice site i, $n_{im} = \sum_\sigma n_{im\sigma}$ with $n_{im\sigma} \equiv b^\dagger_{im\sigma}b_{im\sigma}$ being the number of particle, $\boldsymbol{S}_{im} \equiv b^\dagger_{im\sigma}\boldsymbol{\Gamma}_{\sigma\sigma'}b_{im\sigma'}$ is the total spin operator with $\boldsymbol{\Gamma}_{\sigma\sigma'}$ being the spin matrices for spin-1, $\Theta^\dagger \equiv b^\dagger_{i11}b^\dagger_{i2-1} - b^\dagger_{i10}b^\dagger_{i20} + b^\dagger_{i1-1}b^\dagger_{i21}$, μ_m denotes the chemical potential, and t_m denotes the hopping amplitude between nearest neighboring sites. The U-terms describe the many-body interactions, which are related to the on-site Wannier functions and in principle can be tuned independently in experiments. For example, in general $|U'_m|/U_m \ll 1$ and $|U_{\beta,\gamma}|/U_\alpha \ll 1$ (see experiments in Refs. [34–36]), but these ratios can be tuned via microwave[42,43] or optical Feshbach resonances.[44–51] Notice that U_β describes the interactions between heteronuclear atoms, and is essential for heteronuclear spin exchange during collision, as shown in Refs. [34–36]. We emphasize that this model possesses both features of the Fermi–Hubbard model[31,52,53] and the spinor BH model,[54] due to the allowed odd and even parities. In the following, we mainly focus on the binary mixtures of ^{87}Rb and ^{23}Na with $U_2/U_1 = 1.92$, $U'_1/U_1 = -0.005$ (^{87}Rb), and $U'_2/U_2 = 0.037$ (^{23}Na), and study the interplay of heteronuclear spin-changing U_β and singlet-pairing interactions U_γ.

Heteronuclear Magnetisms from BDMFT. We investigate the system by means of spinor BDMFT, which is nonperturbative and can capture the local quantum fluctuations exactly. For exploring various possible exotic magnetic or superfluid phases, BDMFT has been developed[55] and implemented[16,56–58] successfully for the single-, two-component and spinor Bose–Hubbard models, and the validity of this approach has been verified against quantum Monte–Carlo simulations.[59] See Ref. [41] for more details about this approach. These phases are characterized by various on-site order parameters,[60] including superfluid order $\phi^1_{\sigma m} = \langle b_{m\sigma}\rangle$, spontaneous magnetization $M = |\langle \boldsymbol{S}\rangle|$, spin magnitude $P = \langle \boldsymbol{S}^2\rangle$ (where $\boldsymbol{S} = \boldsymbol{S}_1 + \boldsymbol{S}_2$), nematic order $\phi^2_{\alpha\beta} = \langle S_\alpha S_\beta\rangle - \frac{\delta_{\alpha\beta}}{3}\langle S^2\rangle$ and singlet pairing order $\phi^3_{\text{p}} = \langle \Theta^\dagger\Theta\rangle$. The criteria for these different phases are summarized in Table 1. These orders have also been adopted in other spinor BH models.[15,61,62] We remark here that these order parameters are not orthogonal to each other, thus they may coexist in certain phases. With these order parameters, we characterize the competing Mott phases for $n = 2$ and $n = 3$. Since many parameters are involved in $\hat{H}$, here we are mainly interested in the regimes which can be accessed in experiments.[34–36]

Table 1. Characterization of different quantum phases for heteronuclear mixtures in an optical lattice. The definition of these orders ($\phi^1_{m\sigma}$, $\phi^2_{\alpha\beta}$, ϕ^3_{p}, M, and P) can be found in the main text. The various magnetic orders are not measured (–) in the superfluid (SF) phase with $\phi^1_{m\sigma} \neq 0$.

Phases	$\phi^1_{m\sigma}$	$\phi^2_{\alpha\beta}$	ϕ^3_{p}	M	P
SF	$\neq 0$	–	–	–	–
FM	$= 0$	$\neq 0$	$= 0$	$\neq 0$	$\neq 0$
pFM	$= 0$	$\neq 0$	$\neq 0$	$\neq 0$	$\neq 0$
NI	$= 0$	$\neq 0$	$\neq 0$	$= 0$	$\neq 0$
C	$= 0$	$= 0$	$= 0$	$= 0$	$\neq 0$
SSI	$= 0$	$= 0$	$\neq 0$	$= 0$	$= 0$

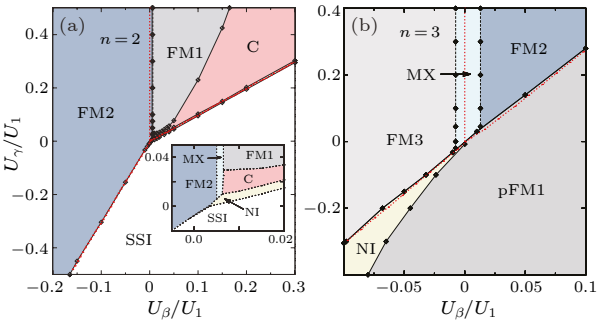

Fig. 1. Phase diagrams for heteronuclear mixtures of spin-1 bosonic gases in a 3D cubic lattice in the typical Mott-insulating regime ($t_{1,2} = 0.01$) for $n = 2$ (a) and 3 (b), respectively. Inset shows the zoom of the main figure near zero U_β/U_1 and U_γ/U_1. Other parameters are $U_2/U_1 = 1.92$, $U_\alpha/U_1 = 1.0$, $U'_1/U_1 = -0.005$ (^{87}Rb), and $U'_2/U_2 = 0.037$ (^{23}Na). Notice that the red dashed lines are from degeneracy analysis. Following the parameters in experiments of Wang's group, we focus on $U_\alpha \sim U_1 \sim U_2$ and $|U'_1| \ll |U_1|$, $|U'_2| \ll |U_2|$ and $|U_{\beta,\gamma}| \ll U_1$.

For $n = 2$ [Fig. 1(a)], we find five different competing phases in the U_γ–U_β plane. When interspecies spin-exchange interaction U_β is large, we can find that the system favors Mott insulating phases with SSI spin order for an even number of atoms per site as a result of the formation of singlet pairs, characterized by $\phi^1_{\alpha 1,2} = 0$, $\phi^2_{\alpha\beta} = 0$, $M = 0$ and $P = 0$. Instead, when the interaction U_β is small, both spins are polarized by paralleling to each other with $M = n$ (FM2). In the intermediate regime with comparable U_β and U_γ, we observe that different types

of spin order compete as a result of competition between spin-exchange and spin-singlet interactions. For examples, FM1, characterized by $M \neq 0$, is energetically favored in the upper part of the panel, but with the two spins being antiparallel to each other. Below this phase, we observe C, characterized by $\phi^1_{\alpha 1,2} = 0$, $\phi^2_{\alpha\beta} = 0$, $\phi^3_{\rm p} = 0$, $M = 0$, and $P \neq 0$. Between the C phase and SSI phase, we also find a narrow regime for nematic insulating (NI) phase, characterized by $\phi^1_{\alpha 1,2} = 0$, $\phi^2_{\alpha\beta} \neq 0$, $\phi^3_{\rm p} \neq 0$, and $M = 0$. While the NI phase has been widely investigated in the spin-1 bosonic particles, we find that this phase is greatly suppressed in our model. Since in our simulations we have essentially considered an infinite system, the small regime for the NI phase should not be attributed to finite-size effects. The experimental regime to observe the NI phase will be discussed in more details in Fig. 4. Note here that forbidden rules $n + M =$ (odd) are allowed for binary mixtures, since the bosonic symmetry of the spin wavefunction on each site is not an indispensable condition for heteronuclear atoms.

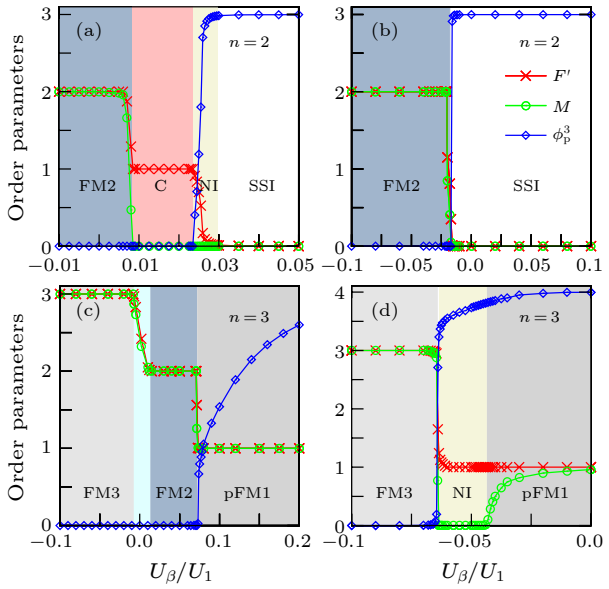

Fig. 2. Zero-temperature phase transitions for mixtures of spin-1 bosons in a 3D optical lattice with filling $n = 2$ and $U_\gamma/U_1 = 0.025$ (a) and -0.05 (b) [Fig. 1(a)], and $n = 3$ and $U_\gamma/U_1 = 0.2$ (c) and -0.2 (d) [Fig. 1(b)].

The order parameters against interaction strengths are presented in Figs. 2(a) and 2(b) for $U_\gamma/U_1 = 0.025$ and -0.05, respectively, which represent attractive and repulsive interactions between the atoms. In the FM2 phase, we find the total magnetization $M = 2$. With the increasing U_β/U_1, a transition from FM2 phase to FM1 (for $U_\gamma > 0$) and SSI phase (for $U_\gamma < 0$) is expected. In the former case we find the magnetization drops from 2 in FM2 phase to 1 in FM1 phase. In the SSI phase, we find that only the singlet pairing order is nonzero with $\phi^3_{\rm p} = 3$ (see Ref. [62], and discussion in Ref. [41]). We find that, the NI phase appears in a small parameter regime between the C and SSI phases, as shown in Fig. 2(a), where the singlet pairing order and nematic order coexist simultaneously with vanishing magnetism. We remark here that the existence of the singlet pairing order ($\phi^3_{\rm p} \neq 0$) is consistent with our single particle analysis, as shown in Ref. [41], and that nematic order $\phi^2_{\alpha\beta}$ is not presented in Fig. 2 to simplify the figure, which is also nonzero for the NI phase. The phase diagram for $n = 3$ is presented in Fig. 1(b), which is totally different from the phase diagram in Fig. 1(a). We can understand these phases from the evolution of order parameters as a function of U_β/U_1 in Figs. 2(c) and 2(d). In the NI phase, we find that the nematic order and singlet pairing order coexist, whereas all these three orders coexist in the pFM1 phase (see the materials in Ref. [41], where we prove that $\phi^3_{\rm p}$ is nonzero only in the regime with $F = 1$ and $g = 3$). Note here that we observe a second-order transition from the NI to the pFM1 phase. The above interesting phases mainly occur in the regime for bosonic particles with odd parity, thus cannot been seen in identical bosonic particles. The whole phase diagrams for heteronuclear atoms are also totally different from the phase diagrams with identical atoms.[61,62] For instance, in two identical atoms, only the C phase can be found in the regime of the FM1 phase with on-site degeneracy $g = 3$. For three identical atoms, the cyclic and trimer phases appear, instead of paired FM1 (pFM1) phase and anti-paralleling FM2 phase (FM2) in the parameter regime studied here. These observations highlight the unique features of heteronuclear mixtures.

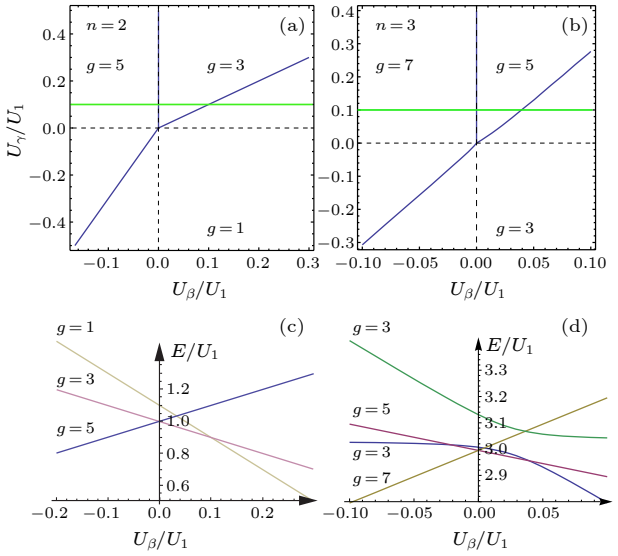

Fig. 3. Parities and degree of degeneracy for two (left) heteronuclear and three (right) heteronuclear atoms in a single well: [(a), (b)] the corresponding phase diagrams, and [(c), (d)] typical eigenvalues as a function of U_β for $U_\gamma/U_1 = 0.1$ [green lines in (a) and (b)].

Heteronuclear Magnetism vs Ground-State Degeneration. Magnetism is formed from the super-exchange interaction between the neighboring sites, which can induce direct coupling between all the quantum states in the degeneracy space. In other words, the ground-state degeneration can be utilized to clarify many-body phase diagrams of the heteronuclear bosonic systems in optical lattices. As shown in Figs. 3(a) and 3(b), the basic structures of phase

diagrams obtained from BDMFT [Figs. 1(a) and 1(b)] can be reproduced by the analysis of ground-state degeneracy. Here, the ground-state degeneracy in each site is given by setting $t_m = 0$, which is presented in Fig. 3. When each site contains two heteronuclear spin-1 atoms ($n = 2$), the angular momentum coupling rule for heteronuclear atoms allows all the possible angular momenta $F = 0$, 1, 2, with the corresponding on-site degeneracy $g = 1$, 3, 5, respectively. The calculated phase diagrams are presented in Figs. 3(a) and 3(c), where the three boundaries are determined by

$$U_\beta = 0, \quad U_\gamma = U_\beta > 0, \quad U_\gamma = \frac{1}{3}U_\beta < 0. \tag{2}$$

These boundaries are independent of U'_m. According to Figs. 1(a) and 3(a), the SSI phase marks the regime when $F = 0$ and $g = 0$, thus the system is simply in the spin singlet insulating (SSI) phase. The spontaneous magnetization can be found when $F = 2$ and $g = 5$, which is denoted as FM2. The phase boundary between SSI phase and FM2 phase is well described by the change of degree of degeneracy at $3U_\gamma = U_\beta < 0$ [see Eq. (2)]. The regime with odd parity ($F = 1$) is most intriguing, due to the possible existence of the cyclic (C) and the ferromagnetic (FM1) phase, which can be tuned by the interaction strengths, although all these phases are created from the same degenerate manifold.

When three atoms ($n = 3$) are occupied in each site, the two identical bosonic atoms admit only even angular momenta, and then the angular coupling between heteronuclear atoms yields $F = 1$, 2, 3 and $F = 1$, with corresponding $g = 3$, 5, 7 and $g = 3$, respectively. The phase boundaries in Fig. 3(b) are determined by

$$\begin{aligned} &U_\beta = 0, \quad 3U_\beta = 4U_\gamma - \sqrt{\Delta} - 9U' > 0, \\ &21U_\beta = 4U_\gamma - \sqrt{\Delta} - 9U' < 0, \end{aligned} \tag{3}$$

where $\Delta = 81U'^2 + 81U_\beta^2 + 48U'U_\gamma + 16U_\gamma^2 - 6U_\beta(27U' + 8U_\gamma)$ when $U' = U'_1$. Different from the boundaries defined in Eq. (2), in this case the boundaries depend strongly on the values as well as the sign of U'_m, without which ($U' = 0$) the two equations collapse to a single line, $U_\gamma = \frac{1}{3}U_\beta$. In the regime when $F = 3$ and $g = 7$, we observe the spontaneous magnetization phase with $M = 3$ (denoted as FM3 phase), while in the regime with $F = 2$ and $g = 5$, we find the similar magnetization phase with $M = 2$ for FM2. Between the FM3 and FM2 phases we find a broad mixed phase (MX) due to the coupling between the $g = 5$ and $g = 7$ degenerate manifolds with closed energies. The similar regime can also be found for $n = 2$ in Fig. 1(a), but this mixed regime is much smaller. Again, the most intriguing regime is for $F = 1$ and $g = 3$, in which the NI phase and paired FM phase, which is now denoted as pFM1 phase, can be realized. The corresponding wave functions for these two cases are supplemented in Ref. [41].

Mott to Superfluid Transitions. We now ask the general question how and where these phases can be found in experiments. Away from the deep Mott-insulating regime, which is frequently encountered in experiments, quantum fluctuations become more and more important with the increase of tunneling amplitudes; until finally the tunneling dominates in the superfluid regime with $\phi^1_{\alpha m} \neq 0$ (see definition in Table 1, and magnetism of weakly interacting bosons can be found in Refs. [30,37–40]). These fluctuation effects can be naturally included in our BDMFT approach.

Our calculated Mott-to-superfluid transition is presented in Fig. 4 for different filling factors. The calculated diagrams depend strongly not only on the tunneling t_m, but also on the values of $U_{\alpha,\beta,\gamma}$ and U'_m. All these spin orders are stable against quantum fluctuations in the Mott-insulating lobes. Phase separation may be found in the $n = 1$ lobe when the two heteronuclear atoms have large difference in tunneling amplitudes and interaction strengths; otherwise, we will find the FM1 or C phase. In the $n = 2$ lobe, we find the SSI, NI and FM2 phases in different parameter regimes. Especially, we find that it is possible to drive the SSI into the NI phase by tuning the tunneling amplitude [see Figs. 4(a) and 4(d)]. While in Fig. 1(a), the NI phase can only be observed in a narrow parameter regime, here we find that this phase can be found in a wide parameter regime by controlling the system parameters. In the $n = 3$ lobe, we find the pFM1 and FM3 phases, while the FM2 phase should be found in other system parameters. These observations demonstrate the experimental observability of the novel magnetic phases predicted in Fig. 1.

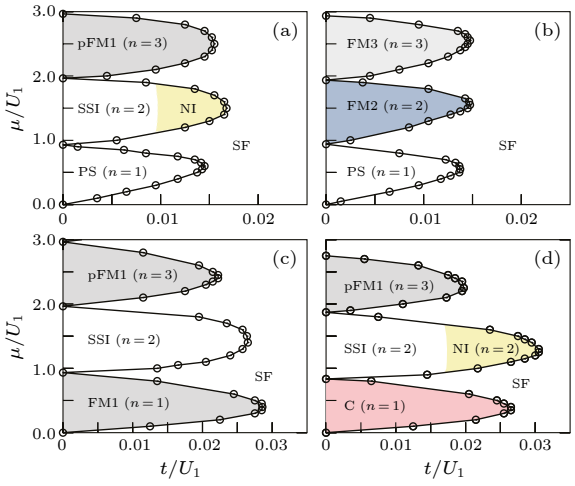

Fig. 4. Mott insulator to superfluid transition of spin-1 heteronuclear atoms in a 3D optical lattice ($t \equiv t_1$). Parameters in (a), (c), and (d) are $U_\beta = 0.032$ and $U_\gamma = 0.0011$ (^{87}Rb and ^{23}Na), while in (b) are $U_\beta = -0.059$ and $U_\gamma = -0.002$. Other parameters are $U_2/U_1 = 1.92$, $t_2/t_1 = 3.78$, $U_\alpha/U_1 = 1.0$ [(a), (b)], $U_2/U_1 = 1.92$, $t_2/t_1 = 1.0$, $U_\alpha/U_1 = 1.0$ (c), and $U_2/U_1 = 1.0$, $t_2/t_1 = 1.0$, $U_\alpha/U_1 = 0.9$ (d). The phase separation phase in (a) and (b) is abbreviated as PS.

We finally discuss the experimental relevance of our theory. Recently, heteronuclear mixtures of spinor ^{23}Na and ^{87}Rb bosonic gases have been realized in an optical dipole trap,[34] and quantum phases of homonuclear spinor ^{23}Na gases in optical lattices explored by overcoming the heating problem induced by the long-time thermalization.[7,63] For this reason, in Figs. 4(a), 4(c), and

4(d) we have adopted the experimental parameters U_β and U_γ for these two atoms, and $U_\alpha^2 < U_1 U_2$ to avoid phase separation. All parameters in the generalized BH model can be tuned independently, for example, the many-body interactions may be tuned via microwave[42,43] or optical Feshbach resonances.[44–51] The microscopic structure of these phases may be detected using Bragg scattering[64] or optical birefringence.[65,66] The gapped spin-singlet insulator has a nonzero gap to all excitations, which can be measured by Bragg scattering, and ferromagnetic phases have a nonzero local spin polarized to a certain direction, which can be measured via spin-dependent light-atom interactions through dispersive birefringent imaging.[65,66] Recently, the spin nematic order in spinor gases was directly measured via a study of the magnetization noise after spin rotation.[67]

In summary, we show that for heteronuclear atoms, the angular momentum composition allows both even and odd parity states even for bosonic atoms, which can give rise to new exotic magnetic phases in the odd parity regimes. We address this issue via the bosonic dynamical mean-field theory approach and map out the complete phase diagrams as a function of many-body interaction strengths, focusing on the $n = 2$ and $n = 3$ Mott lobes. These phases are characterized by magnetization order, nematic order, singlet pairing order, and spin magnitude order, which are determined by not only the on-site degeneracy, but also the competitions from many-body interactions. Their possible relevant regimes and parameters are also presented.

Acknowledgements. We acknowledge useful discussions with Da-Jun Wang, Ying-Mei Liu, Ji-Ze Zhao, and Zeng-Xiu Zhao. This work was supported by the Strategic Priority Research Program of the Chinese Academy of Sciences (Grant No. XDB0500000), the Innovation Program for Quantum Science and Technology (Grant No. 2021ZD0301200), the National Natural Science Foundation of China (Grant Nos. 12074431, 12274384, and 12374252), and the Excellent Youth Foundation of Hunan Scientific Committee (Grant No. 2021JJ10044).

References

[1] Lewenstein M, Sanpera A, Ahufinger V, Damski B, De A S, and Sen U 2007 *Adv. Phys.* **56** 243
[2] Stenger J, Inouye S, Stamper-Kurn D, Miesner H, Chikkatur A, and Ketterle W 1998 *Nature* **396** 345
[3] Schmaljohann H, Erhard M, Kronjäger J, Kottke M, van Staa S, Cacciapuoti L, Arlt J J, Bongs K, and Sengstock K 2004 *Phys. Rev. Lett.* **92** 040402
[4] Barrett M D, Sauer J A, and Chapman M S 2001 *Phys. Rev. Lett.* **87** 010404
[5] Higbie J M, Sadler L E, Inouye S, Chikkatur A P, Leslie S R, Moore K L, Savalli V, and Stamper-Kurn D M 2005 *Phys. Rev. Lett.* **95** 050401
[6] Chang M S, Qin Q S, Zhang W X, You L, and Chapman M S 2005 *Nat. Phys.* **1** 111
[7] Zhao L, Jiang J, Tang T, Webb M, and Liu Y 2015 *Phys. Rev. Lett.* **114** 225302
[8] Gersema P, Voges K K, Borgloh M M Z A, Koch L, Hartmann T, Zenesini A, Ospelkaus S, Lin J, He J, and Wang D 2021 *Phys. Rev. Lett.* **127** 163401
[9] Lin J Y, He J Y, Jin M C, Chen G H, and Wang D J 2022 *Phys. Rev. Lett.* **128** 223201
[10] Huckans J H, Williams J R, Hazlett E L, Stites R W, and O'Hara K M 2009 *Phys. Rev. Lett.* **102** 165302
[11] DeSalvo B J, Yan M, Mickelson P G, de Escobar Y N M, and Killian T C 2010 *Phys. Rev. Lett.* **105** 030402
[12] Taie S, Takasu Y, Sugawa S, Yamazaki R, Tsujimoto T, Murakami R, and Takahashi Y 2010 *Phys. Rev. Lett.* **105** 190401
[13] Krauser J S, Heinze N, Fläschner N, Götze S, Jürgensen O, Lühmann D S, Becker C, and Sengstock K 2012 *Nat. Phys.* **8** 813
[14] Ho T L 1998 *Phys. Rev. Lett.* **81** 742
[15] Demler E and Zhou F 2002 *Phys. Rev. Lett.* **88** 163001
[16] Li Y Q, He L, and Hofstetter W 2016 *Phys. Rev. A* **93** 033622
[17] Koashi M and Ueda M 2000 *Phys. Rev. Lett.* **84** 1066
[18] Santos L and Pfau T 2006 *Phys. Rev. Lett.* **96** 190404
[19] Ho T L and Yip S 1999 *Phys. Rev. Lett.* **82** 247
[20] Cazalilla M A and Rey A M 2014 *Rep. Prog. Phys.* **77** 124401
[21] Kuneš J, Korotin D M, Korotin M A, Anisimov V I, and Werner P 2009 *Phys. Rev. Lett.* **102** 146402
[22] Rizzi M, Rossini D, De Chiara G, Montangero S, and Fazio R 2005 *Phys. Rev. Lett.* **95** 240404
[23] Yip S K 2003 *Phys. Rev. Lett.* **90** 250402
[24] Pollet L 2012 *Rep. Prog. Phys.* **75** 094501
[25] Medley P, Weld D M, Miyake H, Pritchard D E, and Ketterle W 2011 *Phys. Rev. Lett.* **106** 195301
[26] McKay D C and DeMarco B 2011 *Rep. Prog. Phys.* **74** 054401
[27] Mazurenko A, Chiu C S, Ji G, Parsons M F, Kanasz-Nagy M R, Schmidt R, Grusdt F, Demler E, Greif D, and Greiner M 2017 *Nature* **545** 462
[28] Sun H, Yang B, Wang H Y, Zhou Z Y, Su G X, Dai H N, Yuan Z S, and Pan J W 2021 *Nat. Phys.* **17** 990
[29] Xu M Q, Kendrick L H, Kale A, Gang Y Q, Ji G, Scalettar R T, Lebrat M, and Greiner M 2023 *Nature* **620** 971
[30] Luo M, Li Z, and Bao C 2007 *Phys. Rev. A* **75** 043609
[31] Gorshkov A V, Hermele M, Gurarie V, Xu C, Julienne P S, Ye J, Zoller P, Demler E, Lukin M D, and Rey A M 2010 *Nat. Phys.* **6** 289
[32] Honerkamp C and Hofstetter W 2004 *Phys. Rev. Lett.* **92** 170403
[33] Miesner H J, Stamper-Kurn D M, Stenger J, Inouye S, Chikkatur A P, and Ketterle W 1999 *Phys. Rev. Lett.* **82** 2228
[34] Li X K, Zhu B, He X D, Wang F D, Guo M Y, Xu Z F, Zhang S Z, and Wang D J 2015 *Phys. Rev. Lett.* **114** 255301
[35] Wang F D, He X D, Li X K, Zhu B, Chen J, and Wang D J 2015 *New J. Phys.* **17** 035003
[36] Guo M Y, Zhu B, Lu B, Ye X, Wang F D, Vexiau R, Bouloufa-Maafa N, Quéméner G, Dulieu O, and Wang D J 2016 *Phys. Rev. Lett.* **116** 205303
[37] Xu Z F, Zhang Y, and You L 2009 *Phys. Rev. A* **79** 023613
[38] Xu Z, Zhang J, Zhang Y, and You L 2010 *Phys. Rev. A* **81** 033603
[39] Shi Y 2010 *Phys. Rev. A* **82** 023603
[40] Zhang J, Hou X, Chen B, and Zhang Y 2015 *Phys. Rev. A* **91** 013628
[41] See the supplementary material for model details about derivation of extended BH model in Section I, wave functions for $n = 2$ and 3 in Section II, and details about the BDMFT in Section III.
[42] Cheianov V and Chudnovskiy A L 2017 arXiv:1705.01478 [cond-mat.quant-gas]
[43] Papoular D, Shlyapnikov G, and Dalibard J 2010 *Phys. Rev. A* **81** 041603
[44] Hamley C, Bookjans E, Behin-Aein G, Ahmadi P, and Chapman M 2009 *Phys. Rev. A* **79** 023401
[45] Fatemi F, Jones K, and Lett P D 2000 *Phys. Rev. Lett.* **85** 4462
[46] Theis M, Thalhammer G, Winkler K, Hellwig M, Ruff G, Grimm R, and Denschlag J H 2004 *Phys. Rev. Lett.* **93** 123001

[47] Enomoto K, Kasa K, Kitagawa M, and Takahashi Y 2008 *Phys. Rev. Lett.* **101** 203201
[48] Blatt S, Nicholson T, Bloom B, Williams J, Thomsen J, Julienne P, and Ye J 2011 *Phys. Rev. Lett.* **107** 073202
[49] Yamazaki R, Taie S, Sugawa S, Enomoto K, and Takahashi Y 2013 *Phys. Rev. A* **87** 010704
[50] Yan M, DeSalvo B, Ramachandhran B, Pu H, and Killian T 2013 *Phys. Rev. Lett.* **110** 123201
[51] Sándor N, González-Férez R, Julienne P S, and Pupillo G 2017 *Phys. Rev. A* **96** 032719
[52] Kobayashi K, Okumura M, Ota Y, Yamada S, and Machida M 2012 *Phys. Rev. Lett.* **109** 235302
[53] Isaev L, Schachenmayer J, and Rey A M 2016 *Phys. Rev. Lett.* **117** 135302
[54] Belemuk A M, Chtchelkatchev N M, Mikheyenkov A V, and Kugel K I 2017 *Phys. Rev. B* **96** 094435
[55] Byczuk K and Vollhardt D 2008 *Phys. Rev. B* **77** 235106
[56] Hubener A, Snoek M, and Hofstetter W 2009 *Phys. Rev. B* **80** 245109
[57] Hu W J and Tong N H 2009 *Phys. Rev. B* **80** 245110
[58] Anders P, Gull E, Pollet L, Troyer M, and Werner P 2010 *Phys. Rev. Lett.* **105** 096402
[59] Capogrosso-Sansone B, Prokofév N, and Svistunov B 2007 *Phys. Rev. B* **75** 134302
[60] We have verified that all sites are uniform in the parameter regime studied here, and each order parameter in the whole lattice sites takes the identical value within our numerical accuracy. This assumption may break down in fermions (or bosons in other parameter regimes with $n = 1$), due to the formation of antiferromagnetic phases, or in the models with gauge potentials, where the order parameters over more neighboring sites should be defined.
[61] Zhou F and Semenoff G W 2006 *Phys. Rev. Lett.* **97** 180411
[62] Snoek M, Song J L, and Zhou F 2009 *Phys. Rev. A* **80** 053618
[63] Jiang J, Zhao L, Wang S T, Chen Z, Tang T, Duan L M, and Liu Y 2016 *Phys. Rev. A* **93** 063607
[64] Imambekov A, Lukin M D, and Demler E 2003 *Phys. Rev. A* **68** 063602
[65] Natu S S, Pixley J, and Sarma S D 2015 *Phys. Rev. A* **91** 043620
[66] Marti G E and Stamperkurn D 2015 arXiv:1511.01575 [cond-mat.quant-gas]
[67] Zibold T, Corre V, Frapolli C, Invernizzi A, Dalibard J, and Gerbier F 2016 *Phys. Rev. A* **93** 023614